TECHNICAL PROGRESS REPORT

For the Period Ending 3-31-06
(October 1, 2005 to March 31, 2006)

Award Number DE-FC26-03NT41964

Sponsor: DOE Pittsburgh Energy Technology Center

Design, Synthesis, and Mechanistic Evaluation of Iron-Based Catalysis for Synthesis Gas Conversion to Fuels and Chemicals

Akio Ishikawa, Manuel Ojeda, Nan Yao, and Enrique Iglesia
Department of Chemical Engineering
University of California at Berkeley
Berkeley, CA 94720

DISCLAIMER:

ABSTRACT

This project extends previously discovered Fe-based catalysts to hydrogen-poor synthesis gas streams derived from coal and biomass sources. These catalysts have shown unprecedented Fischer-Tropsch synthesis rate, selectivity for feedstocks consisting of synthesis gas derived from methane. During the first reporting period, we certified a microreactor, installed required analytical equipment, and reproduced synthetic protocols and catalytic results previously reported. During the second reporting period, we prepared several Fe-based compositions for Fischer-Tropsch synthesis and tested the effects of product recycle under both subcritical and supercritical conditions. During the third and fourth reporting periods, we improved the catalysts preparation method, which led to Fe-based FT catalysts with the highest FTS reaction rates and selectivities so far reported, a finding that allowed their operation at lower temperatures and pressures with high selectivity to desired products (C_{5+}, olefins). During this fifth reporting period, we have studied the effects of different promoters on catalytic performance, specifically how their sequence of addition dramatically influences the performance of these materials in the Fischer-Tropsch synthesis. The resulting procedures have been optimized to improve further upon the already unprecedented rates and C_{5+} selectivities of the Fe-based catalysts that we have developed as part of this project.

During this fifth reporting period, we have also continued our studies of optimal activation procedures, involving reduction and carburization of oxide precursors during the early stages of contact with synthesis gas. We have completed the analysis of the evolution of oxide, carbide, and metal phases of the active iron components during initial contact with synthesis gas using advanced synchrotron techniques based on X-ray absorption spectroscopy. We have confirmed that the Cu or Ru compensates for inhibitory effects of Zn, a surface area promoter. The kinetic behavior of these materials, specifically the effects of H_2, CO, and CO_2 on the rates and selectivities of Fischer-Tropsch synthesis reactions has led to a new proposal for the nature of rate-determining steps on Fe and Co Fischer-Tropsch catalysts, and more specifically to the roles of hydrogen-assisted and alkali-assisted dissociation of CO in determining rates and CO_2 selectivities. Finally, we have started an exploratory study of the use of colloidal precipitation methods for the synthesis of small Fe and Co clusters using recently developed methods.

During this period, we have had to restrict manpower assigned to this project because some irregularities in reporting and communications have led to the interruption of funding during this period. This has led to less than optimal productivity and to significant disruptions of the technical work. These issues have also led to significant underspending of project funds during this reporting period and to our consequent request for a no-cost extension of one year, which we understand has been granted.

TABLE OF CONTENTS

EXECUTIVE SUMMARY

This project exploits our recent discovery of catalyst compositions and synthesis and activation protocols leading to iron-based catalysts with Fischer-Tropsch synthesis (FTS) rates and selectivities similar to those on cobalt-based catalyst at low temperatures required to form olefins and large hydrocarbons using stoichiometric synthesis gas. These materials are being extended to the conversion of substoichiometric streams to explore whether the unprecedented activities and selectivities with streams derived from natural gas can be realized with more demanding coal-derived synthesis gas ratios. Fe catalysts convert streams derived from coal and biomass, because O-atoms are rejected as CO_2 instead of H_2O, but they tend to be much less active than Co catalysts, which reject O-atoms as H_2O. Fe catalysts are often less stable, because phase transformations can lead to structural disintegration. Higher FTS rates, lower CO_2 selectivities, and greater structural stability remain critical hurdles in converting H_2-poor streams to high-value fuels and chemicals. During the first reporting period, we certified a microreactor, installed required analytical tools, and reproduced previous synthetic protocols and catalytic results. During the second reporting period, we prepared several Fe-based compositions for Fischer-Tropsch synthesis and tested the effects of product recycle under both subcritical and supercritical conditions. During the third reporting period, we improved catalyst synthesis protocols, and achieved the highest FTS reaction rates and selectivities so far reported at the low temperatures required for selectivity and stability. During the fourth and in this fifth reporting period, we have studied the effects of different promoters on catalytic performance, specifically how their sequence of addition dramatically influences the performance of these materials in the Fischer-Tropsch synthesis. The resulting procedures have been optimized to improve further upon the already unprecedented rates and C_{5+} selectivities of the Fe-based catalysts that we have developed as part of this project.

During this fifth reporting period, we have also continued our studies of optimal activation procedures, involving reduction and carburization of oxide precursors during the early stages of contact with synthesis gas. We have completed the analysis of the evolution of oxide, carbide, and metal phases of the active iron components during initial contact with synthesis gas using advanced synchrotron techniques based on X-ray absorption spectroscopy. We have confirmed that the Cu or Ru compensates for inhibitory effects of Zn, a surface area promoter. The kinetic behavior of these materials, specifically the effects of H_2, CO, and CO_2 on the rates and selectivities of Fischer-Tropsch synthesis reactions has led to a new proposal for the nature of rate-determining steps on Fe and Co Fischer-Tropsch catalysts, and more specifically to the roles of hydrogen-assisted and alkali-assisted dissociation of CO in determining rates and CO_2 selectivities. Finally, we have started an exploratory study of the use of colloidal precipitation methods for the synthesis of small Fe and Co clusters using recently developed methods.

During this period, we have had to restrict manpower assigned to this project because some irregularities in reporting and communications have led to the interruption of funding during this period. This has led to less than optimal productivity and to significant disruptions of the technical work. These issues have also led to significant underspending of project funds during this reporting period and to our consequent request for a no-cost extension of one year, which we understand has been granted.

Design, Synthesis, and Mechanistic Evaluation of Iron-Based Catalysis for Synthesis Gas Conversion to Fuels and Chemicals

Description of Tasks

Task One (Years 1 and 2)
Extension of synthesis and activating protocols for Fe-based catalysts prepared by precipitation, treatment with surface-active agents, activation in synthesis gas, and promotion by Ru to materials suitable Fischer-Tropsch synthesis with coal- and biomass-derived synthesis gas.

Task Two (Years 1 and 2)
Characterization of carbide-oxide phase transformations and their impact on catalyst mechanical integrity using electron microscopy and in situ X-ray absorption protocols.

Task Three (Years 2 and 3)
Exploratory studies of the effects of CO_2 and light hydrocarbon recycle on the rate and selectivity of FTS reactions at low H_2/CO ratios on optimized Fe-based catalysts (developed in part (i)).

Objectives and Specific Tasks

Fe-based catalysts are typically preferred for converting coal or biomass derived synthesis gas streams with low H_2/CO ratios (H_2/CO = 0.7-1) because their significant water-gas shift activity ($H_2O + CO \rightarrow CO_2 + H_2$) leads to rejection of excess carbon as CO_2. Fe-based catalysts typically show much lower catalytic activities than Co-based catalysts and lower mechanical stability, as a result of their tendency to interconvert between oxide and carbide phases as the redox properties change within catalytic reactors. Fe-based catalysts with higher Fischer-Tropsch Synthesis (FTS) activity and greater structural integrity remain significant obstacles to their use in the synthesis of high-value fuels and petrochemicals.

Iron-based catalysts with FTS activities and selectivities similar to those on cobalt-based catalyst using stoichiometric H_2/CO streams derived from natural gas were recently reported by our research group. Novel synthesis methods based on supercritical and subcritical drying of powders after precipitation at a constant pH led to significant improvements in the surface area of oxide precursors, while activation and promotion protocols led to active Fe carbide clusters with high surface areas and mechanical strength. These gave in turn unprecedented activity and C_5^+ selectivity during use with stoichiometric synthesis gas (H_2/CO = 2).

The principal objectives of this project are to:

1. optimize synthesis protocols to prepare Fe-based catalysts with FTS rates and hydrocarbon product distributions similar to those of Co-based materials using surface-active compounds and supercritical conditions and explore the use of Ru as activation promoter,

2. evaluate the performance of prepared catalysts in synthesis gas streams derived from coal or biomass (H_2/CO = 0.7-1.0) and optimize activation protocols for high activity, selectivity and mechanical integrity,

3. determine the effects of Ru loading and mode of addition on the concentration of active sites and on the intrinsic activity and selectivity of such active sites,

4. establish the extent and dynamics of carbide-oxide transformations during reactions of synthesis gas mixtures with varying redox potential and their influence on the structural integrity and stability of Fe-based catalysts.

Technical Activities and Accomplishments (FY 2006)

During this fifth reporting period, we have prepared and characterized some Fe-based catalyst and we have measured their Fischer-Tropsch synthesis reaction rates and selectivities. These studies have:

(1) established an appropriate method of iron-based catalysts promotion, resulting in the improvement of the catalytic activity compared to the previous work,
(2) tested and confirmed the high catalytic stability of the samples prepared according to our findings,
(3) shown that the activation of iron-based catalysts at low temperature (508 K) in synthesis gas leads to a more active catalysts than those activated at 523, 543 or 573 K,
(4) demonstrated the promoting effects of Cu (or Ru) and K in enhancing the reduction and carburization of iron oxide precursors and the inhibitory effects of ZnO components used as structural promoters to preserve high surface areas,
(5) performed the evaluation of the performance of prepared catalysts in synthesis gas streams derived from coal or biomass (H_2/CO = 1.0) and optimized activation protocols for high activity, selectivity and mechanical integrity.
(6) determined the kinetic influence of the hydrogen and carbon monoxide partial pressure on catalytic rates and selectivities and propose mechanistic alternatives that can be used for further improvements of Fischer-Tropsch synthesis rates and selectivities
(7) explored the potential use of recently developed colloidal precipitation methods for the synthesis of more active and selective Fischer-Tropsch synthesis catalysts based on Fe and CO.

The detailed results, findings, and conclusions are included in the last part of this report as sections:

2.1. Prepared Catalysts and BET Surface Area.
2.2. Fischer-Tropsch Synthesis on Iron-based Catalysts with Hydrogen-poor synthesis gas.
2.2.1. Effect of promoter order addition on Fisher-Tropsch Synthesis rates and selectivities.
2.2.2. Catalytic performance of Fe-Zn-Cu_3-K_6 in Fischer-Tropsch Synthesis.
2.3. Structure Evolution and Site Requirements in Fe-Catalyzed Fischer-Tropsch Synthesis.
2.3.1. Catalytic behavior of Fe-based catalysts during isothermal activation.
2.3.2. Structural evolution during the activation process.
2.3.2.1 In situ structure and products during reactions on Fe-Zn-Cu_3-K_6 with synthesis gas
2.3.2.2 In situ structure and product evolutions during the catalytic activation process
2.4. Kinetic Study of the Fischer-Tropsch Synthesis on Iron-based Catalyst.
2.4.1. Influence of H_2 partial pressure on reaction rates and product selectivity.
2.4.2. Influence of CO partial pressure on reaction rates and product selectivity.
2.4.3. Mechanism and kinetics of hydrocarbons formation.

Immediate Next Steps and Research Plans

During the next reporting period, we will complete the kinetic study that we began during this reporting period. We will address the detailed kinetic response of optimized catalysts to different reactants partial pressure (H_2, CO, CO_2,). We will optimize and improve the reaction mechanisms reported in this period, and we will derive more rigorous kinetic rate expressions required for scale up in more complex hydrodynamic systems of industrial importance. The detailed comparisons between the experimental data and those predicted with different models will shed light on the reaction mechanism for hydrocarbons formation. We will complete the exploratory study of colloidal synthesis methods at this time. We will also start the assembly of a final report containing all findings of this project.

1. Experimental details

1.1. Synthesis of Precursors and Catalysts

The addition of promoters to Fe-Zn oxide precursors was accomplished following two different procedures, which are shown in Scheme 1. The aqueous solutions of K_2CO_3, $Cu(NO_3)_2$, or ruthenium (III) nitrosylnitrate [$Ru(NO)(NO_3)_x(OH)_y$ (x+y = 3)] were used as the sources of K, Cu and Ru. The first process (Route 1) was carried out according to the previously reported work. First, potassium was added by incipient wetness impregnation with solutions with the required concentration to obtain the desired K/Fe atomic ratio (K/Fe = 0.06). Next the solid was dried overnight at 393 K in ambient air. Cu or Ru were then added at a Cu/Fe and Ru/Fe atomic ratio of 0.03 (Cu(Ru)/Fe = 0.03) in a second step, followed by overnight drying at 393 K in ambient air. Finally, the samples were treated in flowing dry air at 543 K for 4 h. The resulting oxide precursors are denoted throughout as Fe-Zn-K_6, Fe-Zn-K_6-Cu_3, and Fe-Zn-K_6-Ru_3, respectively. The other process (Route 2) was carried out as follows. First, Cu or Ru were added to the Fe-Zn oxide precursor at Cu(Ru)/Fe atomic ratios (Cu(Ru)/Fe = 0.03), followed by overnight drying at 393 K in ambient air and drying at 543 K for 4 h in flowing dry air. Potassium was then added at K/Fe atomic ratios (K/Fe = 0.06) in the second step, followed by overnight drying at 393 K in ambient air. These samples were again treated in flowing dry air at 543 K for 4 h. The resulting oxide precursors are denoted as Fe-Zn-Cu_3-K_6 and Fe-Zn-Ru_3-K_6, respectively.

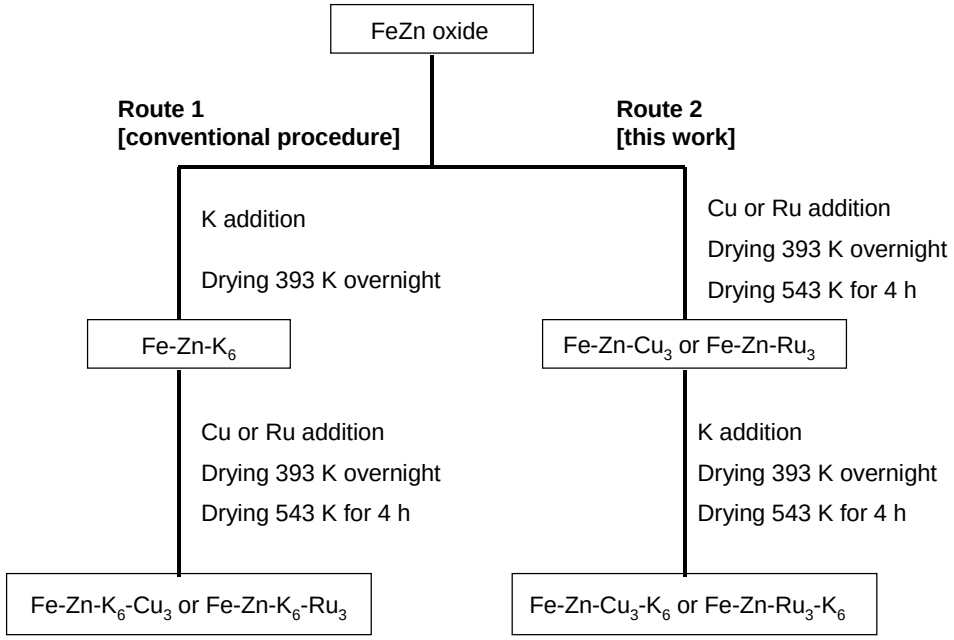

Scheme 1. Procedure for preparation of iron-based catalysts with promoters.

1.2. Fischer-Tropsch Synthesis Reaction and Product Selectivity

Fischer-Tropsch synthesis rates and selectivites were measured in a single-pass packed-bed reactor with plug-flow hydrodynamics. This reactor was held within a resistively-heated three-zone furnace. All lines after the reactor were kept at 433-553 K and a vessel placed immediately after the reactor was held at 408 K to collect liquid products. Reactant and product streams were analyzed online using a gas chromatograph (Agilent Technologies, model 6890N). The analysis of N_2, CO, CO_2, and CH_4 was performed using a thermal conductivity detector and a Porapak Q packed-column (15.2 cm × 0.318 cm diameter). All hydrocarbons up to C_{15} were analyzed on-line using flame ionization detection and a cross-linked methyl silicone capillary column (HP-1, 50 m×0.32 mm; 1.05 μm film).

Fe catalysts (100-180 μ, 0.4 g) were diluted with 11 g of quartz granules (100-180 μ) to avoid temperature gradients. Quartz granules were washed with concentrated nitric acid and treated in air at 973 K before use. Catalysts were activated using flowing synthesis gas (H_2/CO = 2) at 0.1 MPa by increasing the temperature from 298 to 423 K at a rate of 10 K/min and from 423 to 543 K at 1 K/min. The catalysts were held at 543 K for 1 h. After activation, the temperature was decreased to 508 K, and the synthesis gas (H_2/CO = 1) pressure was gradually increased to 2.14 MPa. FTS reactions were carried out with the synthesis gas (Praxair; H_2/CO/N_2 mixture; (i) 0.62/0.31/0.07 [H_2/CO = 2], or (ii) 0.46/0.46/0.08 mol [H_2/CO = 1]) as reactant at 2.14 MPa gas pressure and 508 K.

2. Results and Discussion

2.1. Prepared Catalysts and BET Surface Area

The list of prepared catalysts and BET surface areas are summarized in Table 2.1. The surface area measured by N_2 adsorption at 77 K were 251-291 m^2/g for oxyhydroxide precipitates obtained by drying in ambient air at 393 K. The surface area for Fe-Zn oxides decreased after drying in flowing air at 543 K for 4 h. The addition of K, Cu and/or Ru promoters to Fe-Zn oxides also decreased their surface area, apparently because of pore collapse.

Table 2.1. List of prepared catalysts and BET surface area.

Catalyst	Relative composition (at.)					BET surface area
	Fe	Zn	K	Cu	Ru	m^2/g-cat
FeZn	100	10	-	-	-	198
$FeZnK_6Cu_3$	100	10	6	3	-	141
$FeZnK_6Ru_3$	100	10	6	-	3	147
$FeZnCu_3K_6$	100	10	6	3	-	159
$FeZnRu_3K_6$	100	10	6	-	3	183

2.2. Fischer-Tropsch Synthesis on iron-based catalysts with hydrogen-poor synthesis gas

2.2.1. Effect of promoter order addition on Fischer-Tropsch Synthesis rates and selectivities

The FTS rates and selectivities on the prepared catalysts are shown in Table 2.2. CO conversion rates increased with Ru or Cu addition to Fe-Zn-K, suggesting that Ru and Cu species promote catalyst carburization and reduction rates. This promoter effect can be attributed to a larger number of active sites or to the formation of active sites with a higher intrinsic activity. The rate of CO conversion and hydrocarbon formation was higher on Fe-Zn-Cu_3-K_6 and Fe-Zn-Ru_3-K_6 than on Fe-Zn-K_6-Cu_3 and Fe-Zn-K_6-Ru_3. Those different activities were caused by the two different protocols of promoter addition. Aqueous solutions of $Cu(NO_3)_2$ and $Ru(NO)(NO_3)_x(OH)_y$ were used as sources of Cu and Ru. The pH values for aqueous Cu and Ru complexes solutions were ca. 3 and 0.3, respectively. In the case of Fe-Zn-Cu_3-K_6 and Fe-Zn-Ru_3-K_6, which display high catalytic activities, Cu or Ru were first deposited on the Fe-Zn oxide precursors, dried at 543 K for 4 h in flowing dry air and then K was added. For Fe-Zn-K_6-Cu_3 and Fe-Zn-K_6-Ru_3 samples were obtained by adding of K first and then Cu or Ru. Finally, the catalytic precursors were dried at 543 K for 4 h in flowing dry air. Therefore, this procedure implies that acidic solutions of Cu and Ru solution were added to Fe-Zn oxide and K_2CO_3 particles on the surface of the precursor. It seems that the neutralization reaction of acidic species and K_2CO_3 accompanies this addition of metal nitrate solutions, suggesting that those reactions led to the condensation of Cu or Ru hydroxides and to the decomposition of K_2CO_3. In the case of Fe-Zn-K_6-Cu_3 and Fe-Zn-K_6-Ru_3 samples, it appeared that the condensation of Cu or Ru hydroxides and the decomposition of K_2CO_3 led to higher CH_4, lower C_5^+ selectivity and to lower FTS rates.

The procedure that we propose here for the addition of the catalytic promoters can result in Fe-Zn-Cu_3-K_6 and Fe-Zn-Ru_3-K_6 catalysts with a superior FTS catalytic rates compared to Fe-Zn-K_6-Cu_3 and Fe-Zn-K_6-Ru_3 catalysts prepared by the conventional procedure. Besides, we have found that the Fe-Zn-Cu_3-K_6 catalyst showed the highest FTS performance among all the catalysts here studied.

Table 2.2. Steady-state performance of Fe_2O_3-Zn catalysts (Zn/Fe=0.1) with different loadings of K, Cu, and Ru. (H_2/CO=1, 508 K, 2.14 MPa, CO conversion 12-18%).

	Fe-Zn-K_6	Fe-Zn-K_6-Cu_3	Fe-Zn-Cu_3-K_6	Fe-Zn-K_6-Ru_3	Fe-Zn-Ru_3-K_6
CO conversion rate (mol CO/h.g-at. Fe)	2.2	4.4	6.7	3.2	5.1
Hydrocarbon formation rate (mol CO/h.g-at. Fe)	1.6	3.2	5.1	2.2	3.6
CO_2 selectivity (%)	17.3	28.3	25.9	31.5	30.7
CH_4 selectivity (%) [a]	3.9	2.8	1.9	4.5	2.7
C_5^+ selectivity (%) [a]	84.0	85.7	87.6	80.0	85.5
1-C_5H_{10}/*n*-C_5H_{12} ratio	2.5	2.8	3.1	2.5	2.7

[a] CH_4 and C_5^+ selectivities are reported on a CO_2-free basis.

2.2.2. Catalytic performance of Fe-Zn-Cu_3-K_6 in Fischer-Tropsch Synthesis

The Fischer-Tropsch synthesis was carried on Fe-Zn-Cu_3-K_6 out at 508 K and 2.14 MPa under synthesis gas stream (5.0 NL/h/g-cat.) with $H_2/CO = 1$ for 240 h to examine the stability of this catalytic material. Figure 2.1 shows the dependence of the hydrocarbon formation rate with the time-on-stream (TOS) under synthesis gas ($H_2/CO = 1$). The rate of hydrocarbon formation over Fe-Zn-Cu_3-K_6 decreases rapidly during the initial stages of reaction (ca. 9 h). In this initial period, the sharp decrease in hydrocarbon synthesis rates appears to reflect a decrease of the surface area as a consequence of the carbide-oxide transformations, which take place when synthesis gas contacts the Fe oxide precursors at our reaction conditions (508 K and 2.14 MPa). After this initial period, the hydrocarbon formation rate on Fe-Zn-Cu_3-K_6 decreases gradually and slowly. The following two possibilities can explain this second decrease of the hydrocarbon formation rate. In one case, the catalyst can continuously deactivate as a consequence of the formation of inactive species, such as carbonaceous deposits, on the catalyst surface. In the other case, it is also possible that small amounts of catalyst granules (or even catalytic promoters) are removed out of the reactor by liquid products that leave as such in the trickle-bed operation of these packed-bed reactors. Although the catalyst deactivation by unreactive residues cannot be ruled out, it seems that the decrease of the hydrocarbon formation rate is better explained by the removal of the catalyst (or catalytic promoters) from the catalytic bed. This is supported by the fact that the waxes collected after the reactor display a black color, suggesting that Fe carbides are probably contained within such liquid hydrocarbon streams.

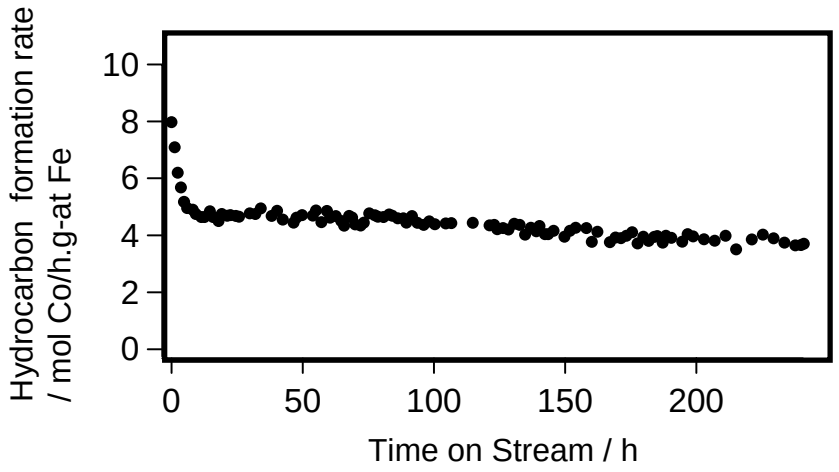

Figure 2.1. Hydrocarbon formation rates with time on stream ($H_2/CO=1$, SV=5.0 NL/h.g-cat) at 508 K and 2.14 MPa.

The improvement of the experimental method may result in more steady FTS rates on Fe-Zn-Cu_3-K_6. Here, we compare FTS reaction rates and selectivities on a Fe-Zn-Cu_3-K_6 catalyst with those on previously reported Fe-based catalysts. Fe-Zn-Cu_3-K_6 samples are compared with the most active reported Fe-based catalysts in Table 2.3 at relatively high CO conversions. CO conversion rates and hydrocarbon synthesis productivities on Fe-Zn-Cu_3-K_6 with a synthesis gas stream containing $H_2/CO = 1.0$ at 508 K are higher than those

reported on Fe-SiO_2-$K_{5.9}$-$Cu_{4.4}$ (H_2/CO = 2.0). The additional investigations of synthesis, promotion and activation protocols in order to increase the density of FTS active site have led to additional improvements in hydrocarbon synthesis productivities.

Table 2.3. Steady State FTS Performance of Various Fe-Based Catalysts Using Natural Gas-Derived Synthesis Gas (H_2/CO = 1.0-2.0).

	Fe-Zn-Cu_3-K_6	Fe-Zn-K_6-Cu_3	Fe-Zn-K_4-Cu_2	Fe-SiO_2-$K_{5.9}$-$Cu_{4.4}$
	This work	Previous work	Ref 1	Ref 2
Reactor Type	Fixed-bed	Fixed-bed	Fixed-bed	Spinning Basket
Temperature (K)	508	508	508	523
Pressure (MPa)	2.14	2.14	2.14	2.4
H_2/CO ratio	1.0	1.0	2.0	2.0
CO conversion (%)	52.2	47.0	50.8	52.7
Hydrocarbon productivity (g/h.kg-cat)	645	415	765	404

Ref 1: S. Li *et al.*, J. Catal. 206 (2002) 202.

Ref 2: van der Laan *et al.*, Ind. Eng. Chem. Res. 38 (1999) 1277.

2.3. Structural Evolution and Site Requirements in Fe-Catalyzed Fischer-Tropsch Synthesis.

2.3.1. Catalytic behavior of Fe-based catalysts during isothermal activation.

During the third reporting period, we reported the FTS performance on several iron-based catalysts under synthesis gas stream at 508 K and 2.14 MPa. Those catalysts were activated at 543 K for 1 h under synthesis gas stream before the FTS reaction was carried out. However, the optimum activation procedure has not been investigated for those catalysts. It is expected that further optimization would lead to even higher FTS rates.

During the fourth reporting period, we examined the structural evolution and site requirements in Fe-Zn-Cu_3-K_6 during activation process.

During this reporting period, we report the obtained results by continuous investigation of the activation procedure.

We have measured the FTS performance on Fe_2O_3, Fe-Zn oxide, and Fe-Zn-Cu_3-K_6 catalysts previously activated under an isothermal activation process (523 K) in order to evaluate the relationship between catalyst activation time and FTS performance. These isothermal activation processes were carried out after treating the samples in He (100 cm^3 min^{-1}) at 573 K for 1 h. Figure 2.2 shows the product formation rates over Fe_2O_3, Fe-Zn oxide, and Fe-Zn-Cu_3-K_6 during the activation process with synthesis gas H_2/CO=2 at 523 K. It can be observed that methane and hydrocarbons are immediately formed on Fe_2O_3, Fe-Zn-Cu_3-K_6 after contact with synthesis gas, and then rates increased with time on stream. This indicates that the active sites on catalysts for FTS reaction were immediately formed after the synthesis gas contact. On the other hand, hydrocarbons are

formed over Fe-Zn oxide after an induction period (ca 5 h). Several iron phases, such as Fe_3O_4 and Fe_3C, have been postulated in the literature to be the active sites for hydrocarbon formation. It seems that the formation of the Fe_3O_4 and Fe carbide phases on Fe-Zn oxide without promoters took place slowly during the induction period, probably because of the Zn effect, that is, Zn seems to inhibit the reduction and carburization of the iron phase. The hydrocarbon and CH_4 formation rates on Fe-Zn oxide increased after ~ 5 h.

After 25 h time-on-stream, the CH_4 formation rate on Fe-Zn oxide was ~ 0.03 mmol/s/g-atom Fe, more than 3 times larger than the methane formation rate on Fe-Zn-Cu_3-K_6. On the other hand, Fe-Zn-Cu_3-K_6 showed the highest C_5^+ selectivity (data not shown). These different FTS selectivities were caused by the presence of potassium promoter.

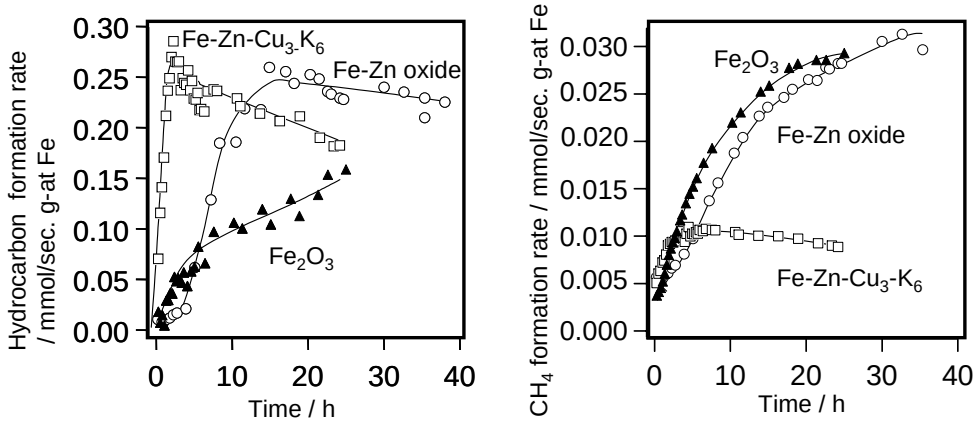

Figure 2.2. CH_4 and hydrocarbon (C_1-C_9) formation rates on iron-based catalysts during activation process. (0.2 g sample; H_2/CO = 2, flow rate: 108 mol/h. g-atom Fe, at 523 K and 0.1 MPa).

Therefore it was found that iron catalysts without promoters need to be activated for more that 20 h. The increase of FTS rates with the reaction time was observed on Fe-Zn-Cu_3-K_6 for ca 5 h after contact with synthesis gas, and then FTS rates decreased with time. It is expected that a further improvement of the activation time brings about the catalyst with higher activity.

2.3.2. Structural evolution during the catalyst activation process.

The structure and nature of the iron oxide phases and the reaction products formed during the catalyst activation process were measured by X-ray absorption spectroscopy and mass spectrometry to explore in detail the behavior of the catalysts during the activation step. The FTS rates on Fe_2O_3, Fe-Zn oxide, and Fe-Zn-Cu_3-K_6, shown in Figure **2.2,** indicate that the catalytic activities on the different catalysts cannot be evaluated on the basis of CH_4 formation rates alone because of the different FTS selectivities among these samples. However, the behavior of CH_4 formation rate for a fixed catalyst can be related to its rate of hydrocarbon formation. Therefore, it seems that the catalytic activity on the same catalyst can be evaluated by its rate of CH_4 formation. In this report, we explored the optimum activation procedure on the basis of the CH_4 formation rate accurately measured by mass spectrometry.

2.3.2.1 In situ structure and products during reactions on Fe-Zn-Cu_3-K_6 with synthesis gas

In situ Fe K-edge X-ray absorption spectroscopy was used to monitor the structural evolution of Fe-Zn-Cu_3-K_6 during activation and FTS reactions. Linear combination method was used to calculate the relative abundance of Fe_2O_3, Fe_3O_4, and FeC_x phases using the near-edge spectral. Figure 2.3 shows the relative various phases required to describe the experimental near-edge spectra during reduction and carburization Fe-Zn-Cu_3-K_6 under synthesis gas stream. The formation of Fe_3O_4 was observed above 373 K, and then the relative abundance of Fe_3O_4 increased, particularly above 450 K. FeC_x formation converted from Fe_3O_4 was also observed above 450 K. The relative abundance of Fe_3O_4 decreased above 560 K, and then FeC_x concentration reached 100% at 580 K. The reduction-carburization reaction of the Fe_2O_3 phase stabilized by ZnO requires the higher temperature as compared to that for pure Fe_2O_3, while Cu decreases the temperature required for the reduction-carburization reaction. The reduction and carburization of Fe-Zn-Cu_3-K_6 occurred at ca 80 K lower temperatures than that of pure Fe_2O_3.

The product formation rates over Fe-Zn-Cu_3-K_6 were obtained by transient FTS experiments at the same reaction condition (H_2/CO = 1, 543 K, 0.1 MPa) as in Figure 2.3. Figure 2.4 shows the product formation rates of CH_4, H_2O and CO_2 during reduction and carburization of Fe-Zn-Cu_3-K_6 under synthesis gas stream. The following reactions are observed during transient FTS experiments; (i) the removal of lattice oxygen atoms from Fe_2O_3 and CuO by H_2 to form H_2O or by CO to form CO_2, (ii) the carburization of iron oxide by CO to form CO_2, (iii) the FT reaction on catalyst by H_2 and CO to form hydrocarbon, H_2O and CO_2, (iv) water-gas shift reaction by CO and H_2O to form CO_2 and H_2. CO_2 formation was observed above 273 K, and then the rate increased with temperature. The H_2O formation rate increased above 450 K, while the CO_2 formation rate decreased concurrently. CuO is not reduced to Cu metal by CO or H_2 at low temperatures near 300 K. The CO_2 formation below ca 450 K assigned to the removal of lattice oxygen atoms from Fe_2O_3 by CO. H_2O formation was observed at temperatures similar to those required for CuO reduction (ca 470 K). H_2O formation includes the reduction of iron oxide via Cu metal by hydrogen as well as the reduction of CuO. XAS results also showed that the Fe_3O_4 formation rate increased above 470 K in Figure 2.3. The formed Cu metal promoted the reduction of Fe_2O_3 to Fe_3O_4 by H_2 which corresponds to the literature. Above 540 K, the CO_2 formation rate and the relative abundance of FeC_x formation dramatically increased, and CH_4 formation was also observed concurrently. Therefore, this CO_2 formation includes the FT reaction on the catalyst as well as the carburization of iron oxide by CO. CO_2 formation rate above ca 620 K assigned to the FT reaction and WGS reaction because the FeC_x concentration already reached 100%. CH_4 formation rates increased with increasing amounts of active sites and reaction temperature. Therefore, it appears that CH_4 formation rates gradually increased with increasing temperature during this experiment. During transient FTS experiments, a temperature above 540 K was required to form CH_4 on the catalyst. Hereafter, the structure and product during catalytic activation process were investigated at temperatures from 508 K (reaction temperature) to 573 K.

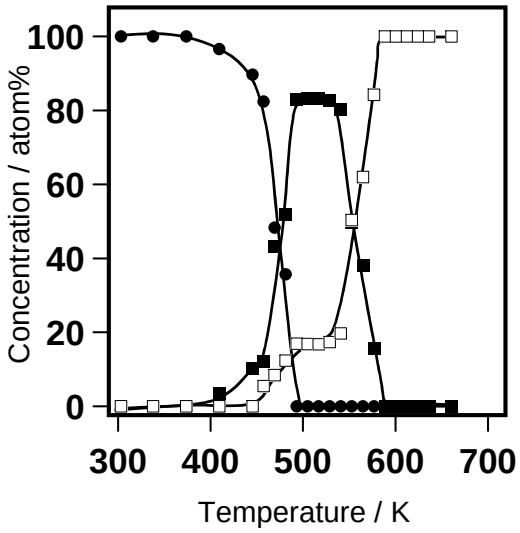

Figure 2.3 In situ evolution of Fe-Zn-Cu_3-K_6 in synthesis gas (H_2/CO=1) as a function of temperature (1 mg of Fe-Zn-Cu_3-K_6, 108 mol/h. g-atom Fe): Fe_2O_3 (circle); Fe_3O_4 (opened square); FeC_x (closed square).

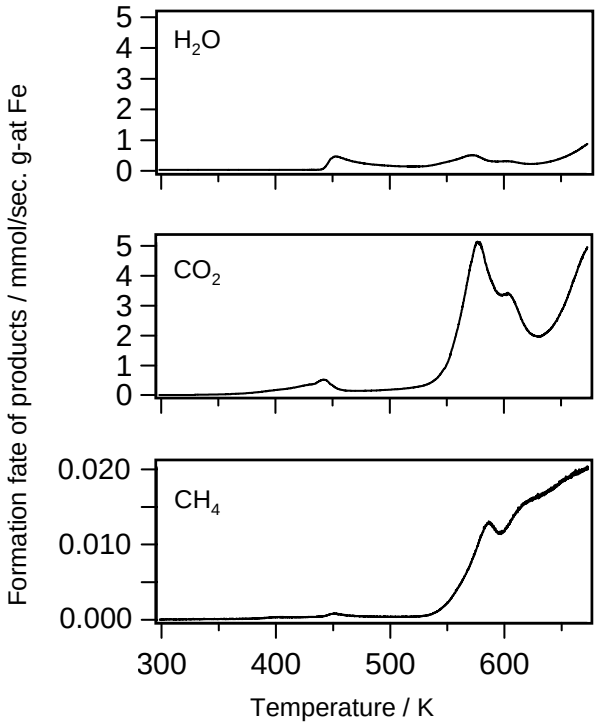

Figure 2.4 Rate of formation of CH_4, H_2O, and CO_2 as a function of temperature on Fe-Zn-Cu_3-K_6 (0.2 g sample). Synthesis gas: H_2/CO = 1, Flow rate: 108 mol/h. g-atom Fe.

2.3.2.2 In situ structure and product evolutions during the catalytic activation process

Figure 2.5 shows the rate of formation of CH_4, H_2O, and CO_2 on Fe-Zn-Cu_3-K_6 catalyst with synthesis gas (H_2/CO = 1, 108 mol/h. g-atom Fe) at 543 K and 0.1 MPa as a function of time on time on stream. Figure 2.5 shows also the concentrations of the Fe_2O_3, Fe_3O_4, and FeC_x phases obtained by near-edge X-ray absorption spectroscopy at the same reaction conditions (H_2/CO = 1, 543 K, 0.1 MPa) during transient FTS experiments. The X-ray absorption spectra of Fe-Zn-Cu_3-K_6 at 543 K changed with time on stream under synthesis gas. The spectra can be described as linear combinations of the near-edge spectra of the three standard compounds (Fe_2O_3, Fe_3O_4, and FeC_x) identified by principal component analysis.

The lattice oxygen atoms are removed from Fe_2O_3 and CuO by H_2 to form H_2O or by CO to form CO_2 during contact with synthesis gas. Carbon is also deposited via CO disproportionation reactions that also form CO_2. Sharp peaks in CH_4, H_2O and CO_2 formation rates were observed after about 1 min of catalyst exposure to synthesis gas at 543 K. The removal of the lattice oxygen from CuO to form Cu metal occurs during this period because the CuO deposited on the catalyst surface is reduced easily to Cu metal at 543 K. However, the amount of removal oxygen during this initial period was larger than that of the lattice oxygen of CuO. X-ray absorption spectra showed that hematite (Fe_2O_3) disappears very quickly during this initial contact with synthesis gas, while Fe_3O_4 and FeC_x species were detected concurrently. The extent of catalyst carburization increased with the reaction time, while the fraction of magnetite (Fe_3O_4) decreased. After 45 minutes on stream, the only iron phase detected was iron carbide (FeC_x). Therefore, the initial exposure of the catalyst to synthesis gas at 543 K also led to the removal of oxygen from the surface and bulk of Fe_2O_3 to form Fe_3O_4 and finally, to the introduction of carbon into the iron structure to form FeC_x. This latter process is very fast, as indicated by the observation that the concentration of FeC_x reached 20% after 1 min.

The carburization of an Fe oxide is an exothermic reaction. This is supported by the increase of the reaction temperature that we observed after the initial contact between the synthesis gas and the catalyst. The increase of the catalyst temperature as a result of the sudden formation of the FeC_x species at the beginning of the reaction (1 min) seems to be the reason of the sharp peaks corresponding to the formation of CH_4, H_2O and CO_2 in Figure 2.5.

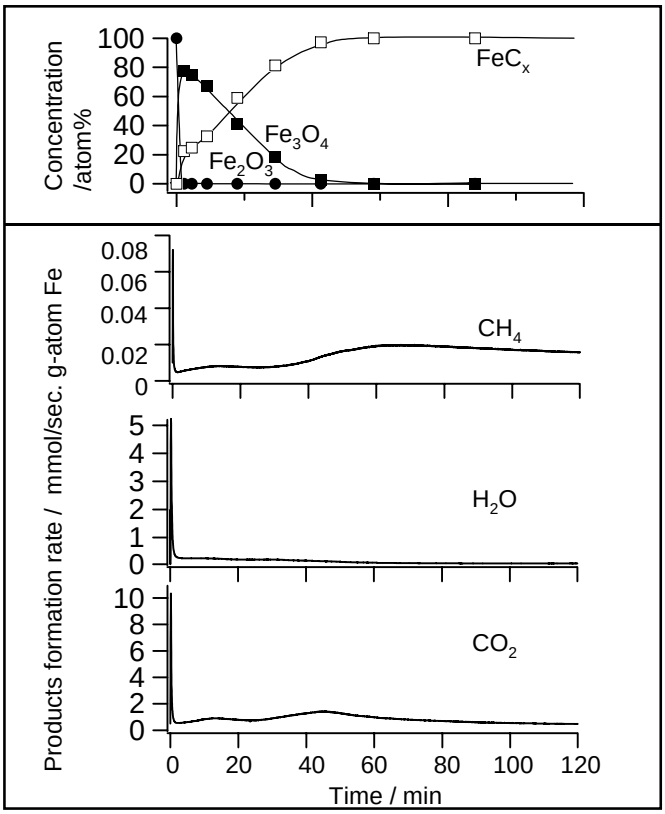

Figure 2.5 Structural evolution obtained from XAS (1 mg sample, 543 K) and rate of formation of CH_4, H_2O, and CO_2 as a function of time on Fe-Zn-Cu_3-K_6 (0.2 g sample, 543 K). Synthesis gas: H_2/CO = 1, Flow rate: 108 mol/h. g-atom Fe.

As described earlier, a sharp peak corresponding to the rate of water formation is observed initially. Subsequently, the water formation rate decreased with time on stream. The behaviors of CH_4 and CO_2 formation rates are different. In this case, two broad formation rate peaks were observed. The first CO_2 formation rate is attributed to the reduction of hematite to form magnetite, while the second peak is the consequence of the formation of iron carbides. The surface area of Fe-Zn-Cu_3-K_6 was 160 m^2/g, while those of samples after 25 and 70 minute contact with synthesis gas were 31 and 27 m^2/g respectively. It was markedly clear that the Fe-Zn-Cu_3-K_6 sample rapidly sintered during the Fe_3O_4 formation due to the similarity of the skeletal density of Fe_3O_4 (5.2 g/cm^3) to that of Fe_2O_3 (5.2 g/cm^3). The surface area also decreased during the conversion of Fe_3O_4 to FeC_x, even with the higher skeletal density of Fe_3C (7.7 g/cm^3). This result demonstrates that the sample slowly sintered on each particle. It is likely that the first broad peak of the CH_4 formation rate is mainly attributed to the CH_4 formation on Fe_3O_4 species, which would indicate that Fe_3O_4 is also an active species for the Fischer-Tropsch reaction. The other methane formation rate peak is attributed to the CH_4 formation on FeC_x species. The rate of CH_4 formation reached the maximum value when the FeC_x concentration reached 100%, and then decreased slowly with time.

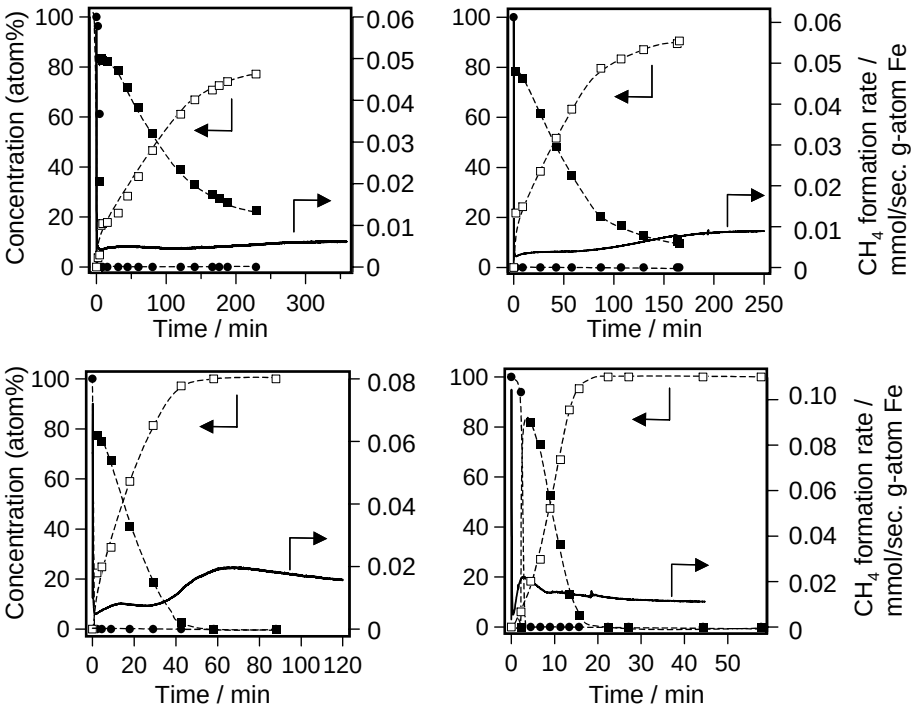

Figure 2.6 Fe carbide concentration (open mark) obtained from XAS (1 mg sample) and rate of formation of CH_4 as a function of time on Fe-Zn-Cu_3-K_6 (0.2 g sample) at (a) 523, (b) 543 and (c) 573 K. Synthesis gas: H_2/CO = 1, Flow rate: 108 mol/h. g-atom Fe.

Figure 2.6 shows the iron carbide concentrations obtained from *in situ* XAS on Fe-Zn-Cu_3-K_6 as a function of time at different reaction temperature. It can be observed that at 543 and 573 K, FeC_x contributions approached constant values of ca. 100% after 60 and 20 min respectively. On the other hand, the FeC_x contributions at 508 and 523 K were ca 80% and ca 90% after 360 and 180 min, respectively. Figure also shows the CH_4 formation rates measured at the same reaction condition as those used for the XAS experiments. The rate of CH_4 formation at 508 and 523 K increased with increasing FeC_x content. At 543 and 573 K, the CH_4 formation rates increased with increasing FeC_x content and then the rates decreased with time on stream. At 573 K, the deactivation of the catalyst took place after 5 minutes in contact with synthesis gas. It seems that the decrease of CH_4 formation rates was caused by the formation of the inactive species, such as carbon, upon exposing the iron oxide to synthesis gas at high temperature. It was found that the deactivation of catalyst accompanied the activation process at high temperature.

FTS rates increase with increasing reaction temperature. To evaluate the optimum activation process by the CH_4 formation rate, it is necessary to measure this rate of CH_4 formation at the same conditions after the activation process. Table 2.4 summarizes the surface area of Fe-Zn-Cu_3-K_6 activated at various temperatures as well as the CH_4 formation rates measured at 508 K after different activation processes. The activation processes at 543 and 573 K were carried out for 70 and 5 min, respectively, because according to Figure 2.6, the Fe-Zn-Cu_3-K_6 catalyst needs to be activated for these periods of time in order to achieve the highest rate of CH_4 formation. The surface area of Fe-Zn-Cu_3-K_6 activated at 508 K for 360 min was the lowest value among all the samples and the

FeC_x concentration was 80%. It seems that the activation at high temperature leads to the preferential nucleation of a new phase at multiple locations on the surface of an Fe_2O_3 crystallite because of the rapid reduction and carburization of the catalysts. Therefore, it appears that the increase of activation temperature results in the increase of the surface area. However, the Fe-Zn-Cu_3-K_6 activated at 508 K for 360 min showed the highest CH_4 formation rate, despite the fact that this sample displayed the lowest surface area and lowest FeC_x concentration. There are apparently two possibilities in order to explain this behavior. One of them is the rapid deactivation of catalyst activated at high temperature. The contact Fe-Zn-Cu_3-K_6 with synthesis gas at 573 K brought about the deactivation of catalyst just after 5 min in spite of the low FeC_x concentration (20%). The other possibility is that active sites formed via promoters have the satisfactory promoter effects. Cu and K species on the Fe_2O_3 surface promote the reduction and carburization of Fe_2O_3. The reduction and carburization of the Fe-Zn-Cu_3-K_6 catalyst at low temperature takes place because of the presence of the different promoters, while the reduction and carburization at high temperature, particularly at 573 K, takes place more easily, even without the presence of promoters. Therefore, at the higher temperatures, the reduction and carburization by H_2 and CO caused the lack of promoter effect on the formation of the active species during the reduction and carburization processes. According to our results, it appears that the Fe-Zn-Cu_3-K_6 catalyst activated at low temperature (508 K) with satisfactory promoter effects showed the highest CH_4 formation rate.

Table 2.4. Characterization results and CH_4 formation rate over Fe-Zn-Cu_3-K_6 activated a different temperature and time.

Temperature (K)	508	523	543	573
Activation time (min)	360	300	70 (120)	5 (45)
surface area after reaction (m^2/g)	13.1	14.6	26.9 (16.8)	42.5 (31.3)
Steady-state FeCx [a] concentration (%)	80	90	100 (100)	20 (100)
Steady-state CH_4 formation [b] rate (mmol/sec. g-atom Fe)	0.0060	0.0054	0.0052 (0.0047)	0.0039 (0.0031)

[a] FeC_x concentration measured after exposure to synthesis gas (1 mg Fe-Zn-Cu_3-K_6, H2/CO = 1, synthesis gas flow rate = 108 mol/h. g-atom Fe)

[b] CH_4 formation rates measured at 508 K after activation at various temperatures (0.2 g Fe-Zn-Cu_3-K_6, H_2/CO = 1, synthesis gas flow rate = 108 mol/h. g-atom Fe)

Up to this point, the activation procedure has been carried out systematically at 543 K for one hour. However, these activation conditions have not been optimized in spite of the importance of this process to optimum FTS reactions. Our results suggest that catalyst activation at low temperature has a positive effect on its catalytic performance.

FT performance were measured over Fe-Zn-Cu_3-K_6 samples with hydrogen-poor synthesis gas (H_2/CO = 1) reactant. The Fe-Zn-Cu_3-K_6 samples were activated with stoichiometric synthesis gas (H_2/CO = 2) reactant at 508 K and three flow rates [(i) 21.6, (ii), 54.0 (iii) 108 mol/h.g-atomFe] before FT performance measurements. The flow rate (108 mol/h.g-atomFe) had the same value as that of transient FTS experiments. Table 2.5

summarizes the steady-state performance of Fe-Zn-Cu_3-K_6 activated at 508 K and several synthesis gas flow rates. Here, Table 2.5 also shows the steady-state performance of Fe-Zn-Cu_3-K_6 activated by conventional method [543 K, 21.6 mol/h.g-atomFe].

The decrease of flow rate during the activation process led to the increase of the CO conversion rate and the hydrocarbon formation rate as well as the increase of CO_2 and CH_4 selectivities. In the case of fast synthesis gas flow (108 mol/h.g-atm Fe), it is possible that a small amount of catalytic promoter and catalysts granules are removed out of the reactor during the rapid structure change. Cu promoter increases CH_4 and CO_2 selectivities and decreases C_5^+ selectivity.[ref] Therefore, it seems that the effects of Cu promoter increased with decreasing the synthesis gas flow rate.

The Fe-Zn-Cu_3-K_6 activated with synthesis reactants (H_2/CO=2, flow rate 21.6 mol/h.g-at Fe) at 508 K showed the highest FT performance among all catalysts. The suggested optimum activation process improved the FT performance of Fe-Zn-Cu_3-K_6 under FT condition (508 K, 2.14 MPa, hydrogen-poor synthesis gas reactant [H_2/CO=1]).

Table 2.5 Steady-state performance of Fe-Zn-Cu_3-K_6 activated at several conditions. (H_2/CO=1, 508 K, 2.14 MPa, CO conversion 29-32%)

Activation Temperature (K)	543	508	508	508
Flow rate (mol/h.g-atomFe)[a]	21.6	21.6	54.0	108
steady-state performance at 508 K, 2.14 MPa, synthesis gas (H_2/CO=1)				
CO_2 selectivity (%)	29.5	35.3	34.6	31.4
CH_4 selectivity (%)[b]	4.9	4.8	4.1	3.9
C_5^+ selectivity (%)[b]	86.1	88.3	90.2	90.2
CO conversion rate (mol CO/h.g-at. Fe)	6.31	7.08	6.89	6.54
Hydrocarbon formation rate (mol CO/h.g-at. Fe)	4.45	4.58	4.50	4.49

[a] Synthesis gas (H_2/CO=2)

[b] CH_4 and C_5^+ selectivities are reported on a CO_2-free basis.

2.4. Kinetic Study of the Fischer-Tropsch Synthesis on Iron-Based Catalyst.

The kinetics of the Fischer-Tropsch Synthesis (FTS) have been studied during this reporting period. The kinetic measurements have been performed on Fe-Zn-Cu_3-K_6, which was found to be the most active catalyst in previous studies. The ultimate objective of these experiments is to propose a reaction mechanism that describes and predicts the rates of formation of the various hydrocarbons formed during reactions of CO and H_2 on Fe-based catalysts and which can be used to embed into hydrodynamic models of complex practical reactors.

In the previous report, the influence of hydrogen, carbon monoxide and carbon dioxide partial pressures on the reaction rates over a Fe-Zn-Cu_3-K_6 catalyst were presented. During this reporting period, a reaction mechanism in agreement with the experimental data has

been proposed. By applying the pseudo-steady-state hypothesis (PSSH), kinetic expressions corresponding to the formation of hydrocarbons, water and primary CO_2 have been derived. The proposed mechanism and kinetic equations are in good agreement with the experimental data, describing and predicting the rates of formation of the various hydrocarbons formed during reactions of CO and H_2 on Fe-based catalysts.

2.4.1. Influence of H_2 partial pressure on reaction rates and product selectivity.

We have measured the influence of hydrogen and carbon monoxide partial pressures over the catalytic performance of Fe-Zn-Cu_3-K_6 at 508 K. Figure 1.1 shows the influence of CO and H_2 partial pressures on the CO conversion rate to hydrocarbons at different values of CO space velocity. It can be seen that hydrocarbons formation rate increases by increasing both CO and H_2 pressures.

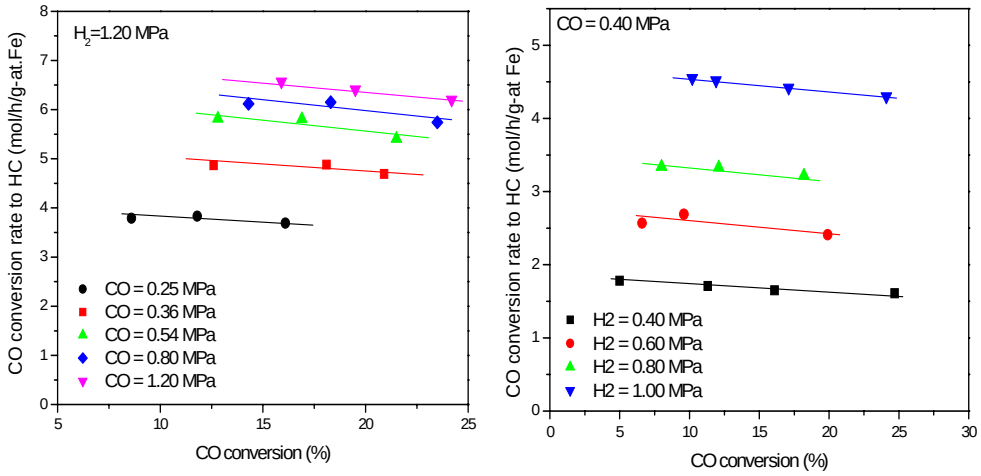

Figure 2.7. Influence of CO (left) and H_2 (right) partial pressures on the CO conversion rate to hydrocarbons over Fe-Zn-Cu_3-K_6 at different values of CO space velocity.

Figure 2.7 shows the influence of reactants partial pressure over the forward CO_2 formation rate. The slopes of the CO_2 formation rate, which give a measure of the contribution of the rate of secondary CO_2-forming reactions, increased very slightly with increasing inlet CO partial pressure. The forward rate of CO_2 formation extrapolated to very low CO conversion levels are non-zero, consistent with the primary CO_2 formation *via* the reaction of chemisorbed carbon monoxide (CO*) and chemisorbed oxygen (O*). It is evident that main effect of increasing inlet CO partial pressures on CO_2 formation pathways is to enhance this primary CO_2 formation rate. On the other hand, the intercept with the y-axis at very low CO conversion levels and the slopes of the forward CO_2 formation rate are independent of the inlet H_2 partial pressure, which means that hydrogen does not affect the rate of primary oxygen atoms removal pathway as CO_2 or the carbon dioxide formation through the water-gas shift reaction.

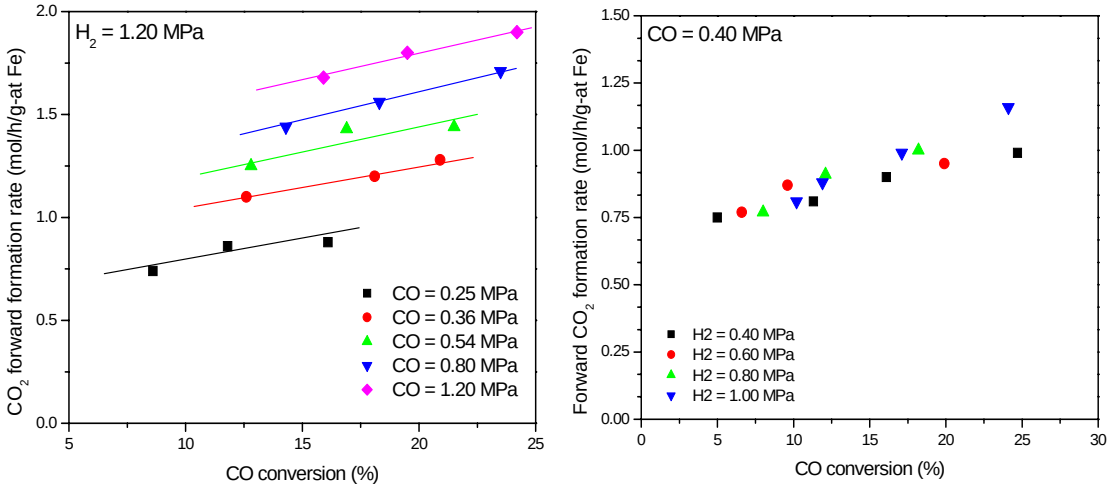

Figure 2.8. Influence of CO (left) and H_2 (right) partial pressures on the forward CO2 formation rate over Fe-Zn-Cu_3-K_6 at different values of CO space velocity.

2.4.2. Influence of CO_2 partial pressure on reaction rates and product selectivity.

From our experimental results, we have extended the previous study of the Fischer-Tropsch Synthesis mechanism and kinetics. In this reporting period, we propose a set of elementary steps taking into consideration the formation of hydrocarbons and CO_2 through primary pathways. The observed kinetic dependence of rates of hydrocarbons and primary CO_2 formation on the reactants partial pressures led us to propose the following set of elementary steps for the Fischer-Tropsch Synthesis:

1. $CO + * \rightleftharpoons CO*$
2. $H_2 + 2* \rightleftharpoons 2\ H*$
3. $CO* + H* \rightleftharpoons COH* + *$
4. $COH* + H* \longrightarrow CH* + H*$
5. $CO* + * \longrightarrow C* + O*$
6. $C* + H* \longrightarrow CH* + *$
7. $CH* + H* \longrightarrow CH_2* + *$
8. $OH* + H* \longrightarrow H_2O + 2*$
9. $CO* + O* \longrightarrow CO_2 + 2*$

Scheme 2.1. Proposed elementary steps for hydrocarbons (CH_2* species), water and primary carbon dioxide formation from CO and H_2.

The corresponding kinetic expressions obtained for the formation of hydrocarbons and primary carbon dioxide by applying the pseudo-steady-state hypothesis (PSSH) to the intermediates are presented in Table 2.6. A nonlinear regression method has been used to fit the experimental data to the different rate expressions. The model parameters were calculated from the experimental data by using the Levenberg-Marquardt method with all experimental reaction rates.

Table 2.6. Rate expressions and parameters for the FTS kinetic model.

Rate Expression	r^2	$K_1K_2K_3k_4$ (MPa^{-2})	K_1k_5 (MPa^{-1})	K_1 (MPa^{-1})
$r_{HC} = \frac{K_1K_2K_3k_4 P_{CO}P_{H2} + K_1k_5 P_{CO}}{(1+K_1P_{CO})^2}$	0.983	16.05±1.04	2.70±0.44	0.84±0.09
$r_{H_2O} = \frac{K_1K_2K_3k_4 P_{CO}P_{H2}}{(1+K_1P_{CO})^2}$	0.992	15.68±1.59	-	0.78±0.11
$r^p_{CO_2} = \frac{K_1k_5 P_{CO}}{(1+K_1P_{CO})^2}$	0.973	-	3.47±0.82	0.68±0.23

Figures 2.9, 2.10 and 2.11 compare the experimental and the calculated rates of hydrocarbons, primary CO_2 and water formation respectively. It is observed that the reaction rates calculated with the kinetic expressions derived from our model are in good agreement with the experimental values.

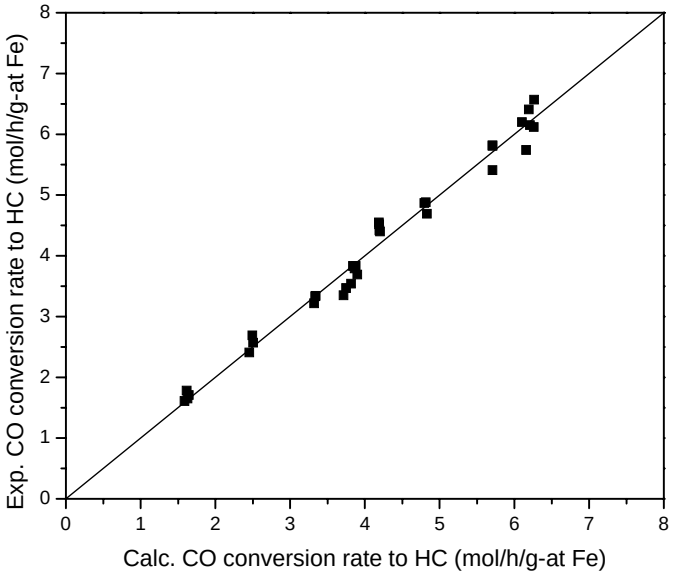

Figure 2.9. Parity plot for the experimental and calculated CO conversion rate to hydrocarbons.

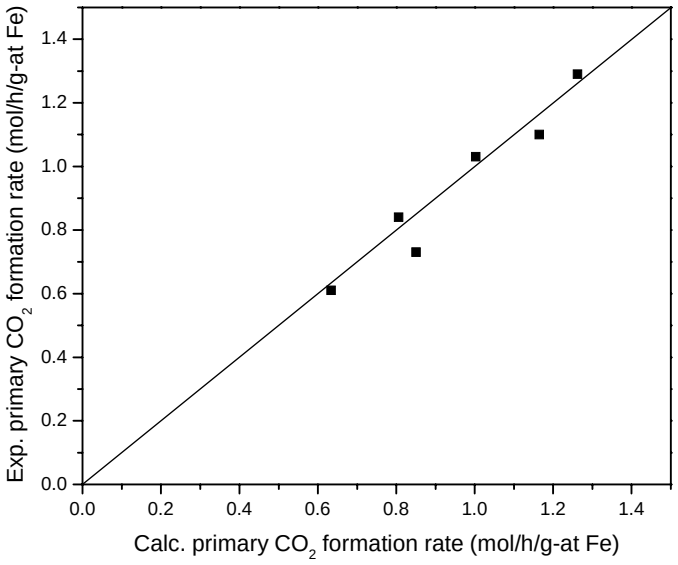

Figure 2.10. Parity plot for the experimental and calculated forward CO_2 formation rate.

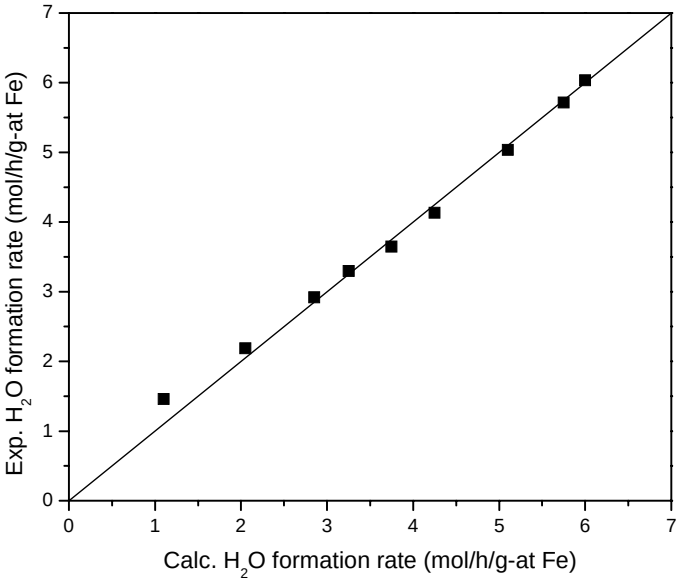

Figure 2.11. Parity plot for the experimental and calculated water formation rate.

In this study, we contemplate the possibility of parallels pathways for CO activation over Fe catalysts. On one hand, adsorbed CO* species can be directly dissociated to form surface carbon atoms which can be subsequently hydrogenated to produce the FTS monomers (CH_2*). But at the same time, hydrogenation of carbon monoxide molecules associatively adsorbed also lead to the formation of surface monomers. Both monomer formation routes occur simultaneously over the catalyst surface, although the hydrogen-assisted CO dissociation mechanism is predominant under our reaction conditions. The hydrocarbons formation rate expression reflects the contribution of both pathways.

From Table 2.6, it is derived that the formation of water should be about five times faster that the formation of primary carbon dioxide at constant H_2 partial pressure, which means that CO dissociation with hydrogen assistance should take place about five times more

rapidly than the direct C-O bond splitting. This is supported by the experimental results (Figure 2.12), which shows that the r_{H2O}/r_{CO2} ratio is about 5.

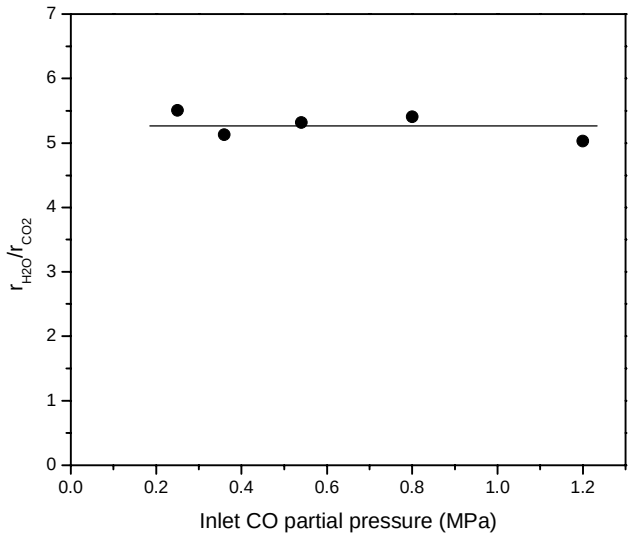

Figure 2.12. Water-to-carbon dioxide formation rate ratio extrapolated at zero CO conversion as a function of the inlet CO pressures (P_{H2}=1.20 MPa).

2.4.3. Mechanism and kinetics of hydrocarbon formation.

The reaction mechanism proposed in this work can also be extrapolated to cobalt-based catalysts, leading to some differences between the pathway of hydrocarbons formation with cobalt and iron catalysts. It is well known that cobalt-based FTS catalysts do not form carbon dioxide (1), which is in contrast to the behavior of iron-based FTS catalysts. This different property strongly suggests that hydrocarbons formation with cobalt catalysts does not occur *via* direct CO dissociation and that hydrogen assistance in the carbon monoxide dissociation plays the main role. It is mostly agreed that steps involving the hydrogenation of surface carbonaceous species are the kinetically relevant ones in the FTS with cobalt catalysts (2, 3). However, it is uncertain if the rate determining step is the addition of hydrogen to surface carbon atoms (C* + H* → CH*) or to partially hydrogenated species (CH* + H* → CH_2*). The controversy still persists in the literature (4-7). The proposal of the latter elementary step as the rate-determining one is mainly related to the fact of the experimentally first order of the FTS reaction with respect the hydrogen partial pressure (3, 8). It has been suggested that the hydrogenation of surface carbon (C*) and of CH* species are mainly irreversible (4). Therefore, it is unlikely to think that the hydrogenation of CH* species is rate limiting.

A uniformly applicable rate expression for cobalt catalysts has not yet been found (9). Yates and Satterfield (10) proposed a Langmuir-Hinshelwood type equation which described accurately their results:

$$-r_{CO} = \frac{k P_{CO} P_{H_2}}{(1 + K P_{CO})^2}$$

The same equation was previously derived by other authors (11) assuming hydrogenation of adsorbed formyl to form carbon and water to be rate-limiting. Since carbon dioxide formation is not detected with cobalt catalysts, it can be assumed that CO activation takes place exclusively *via* hydrogen assistance (Scheme 1.1, steps 3 and 4). In this case, the equation for hydrocarbons formation that we proposed over Fe-based catalysts in Table 1.1 can be simplified. The resulting expression is similar to that published in the literature for cobalt catalysts (10).

In conclusion, we have find a general mechanism for the Fischer-Tropsch Synthesis which is independent on the type of catalyst used (iron or cobalt). In both cases, hydrocarbons are mainly formed from surface species obtained *via* CO dissociation with hydrogen assistance. The alternative pathway for CO activation *via* direct dissociation does not contribute significantly to the formation of the desired hydrocarbons over cobalt catalysts, although this mechanism becomes more important over iron-based catalysts.

References

1. M.J. Keyser, R.C. Everson, R.L. Espinoza, Ind. Eng. Chem. Res. 39 (2000) 48.
2. M.E. Dry, Catal. Today 6 (1990) 183.
3. A.O.I. Rautavuoma, S. van der Baan, Appl. Catal. 1 (1981) 247.
4. E. van Steen, H. Schulz, Appl. Catal. A: Gen. 186 (1999) 309.
5. H.A.J. van Dijk, J.H.B.J. Hoebink, J.C. Schouten, Topics Catal 26 (2003) 111.
6. J. Panpranot, J.G. Goodwind, Jr., A. Sayari, J. Catal. 213 (2001) 78.
7. P. Biloen, J.N. Helle, W.M.H. Sachtler, J. Catal. 58 (1979) 95.
8. E. Iglesia, S.C. Reyes, R.J. Madon, S.L. Soled, Adv. Catal. 39 (1993) 221.
9. R.L. Espinoza, Prep. Am. Chem. Soc., Fuel Div. 40 (1995) 172.
10. I.C. Yates, C.N. Satterfield, Energy and Fuels 5 (1991) 168.
11. B. Sarup, B.W. Wojciechowski, Can. J. Chem. Eng. 67 (1989) 62.

2.5. Bimetallic Colloids for Fischer-Tropsch Synthesis Catalysts

2.5.1. CoRu bimetallic colloid preparation and support on ZrO_2/SiO_2

We have recently started an exploratory study of the use of colloidal precipitation methods for the synthesis of small Fe and Co clusters using recently developed methods. The general scheme and approach is shown below for Co-Ru catalysts and it is being extended to cover the synthesis of Fe-based catalysts.

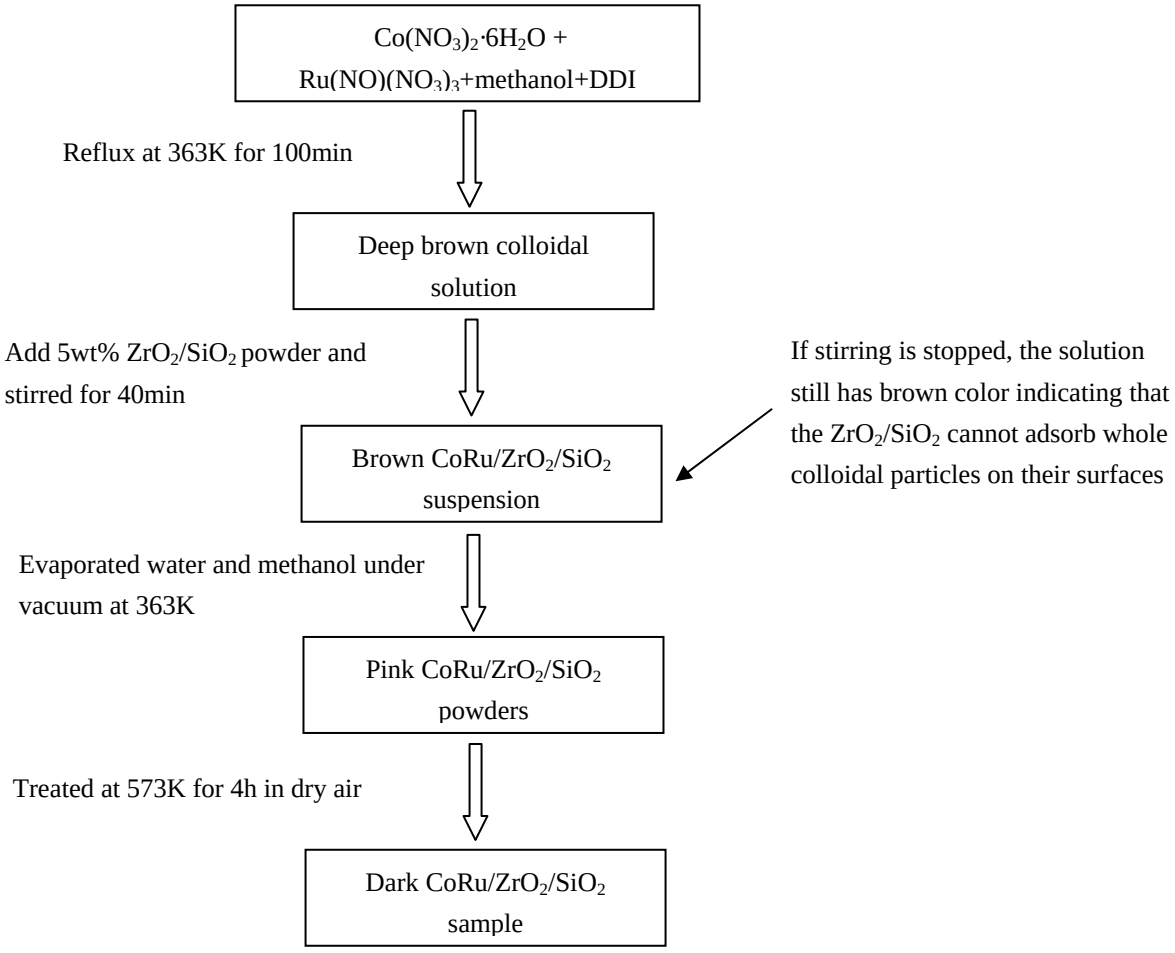

SB12 [3-(N,N-dimethyldodecylammonio)-propanesulfonate] was used as surfactant to stabilize the colloidal particles.

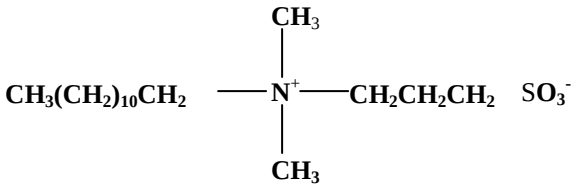

Figure 2.5.1 Preparation process of a CoRu catalyst via colloidal precursor

Appendix B:

1. Publications

1.1 A manuscript titled “Fischer-Tropsch synthesis on iron-based catalysts with hydrogen-poor synthesis gas” is currently under review by Prof. Iglesia and will be submitted for publication.

1.2 A manuscript titled “Structure Evolution and Spectroscopic Studies of Site Requirements in Iron-Catalyzed Fischer-Tropsch synthesis” is currently in preparation and will be submitted for publication.

1.3. A manuscript titled “A kinetic and mechanistic study of the Fischer-Tropsch Synthesis with Fe-based catalysts” is currently under review by Prof. Iglesia and will be submitted for publication.

2. Presentations and Abstracts

2.1. Akio Ishikawa, Manuel Ojeda, Enrique Iglesia, “Design, Synthesis and Catalytic Properties of Iron-Based Catalysts for the Synthesis Gas Conversion to Fuels and Chemicals”, The Fifth Tokyo Conference on Advanced Catalytic Science and Technology (TOCAT 5), July 23 -28, 2006 (See Abstracts below)

2.2. Manuel Ojeda, Akio Ishikawa, Enrique Iglesia, “Iron-Catalyzed Fischer-Tropsch Synthesis: Mechanism and Catalyst Optimization”, AIChE 2006 Annual Meeting San Francisco, November 12-17, 2006 (See Abstracts below)

Abstract submitted to "The Fifth Tokyo Conference on Advanced Catalytic Science and Technology (TOCAT 5)" July 23 -28, 2006

Design, Synthesis and Catalytic Properties of Iron-Based Catalysts for the Synthesis Gas Conversion to Fuels and Chemicals

Akio ISHIKAWA, **Manuel OJEDA, Enrique IGLESIA***

Department of Chemical Engineering, University of California, Berkeley, CA 94720, USA

Tel :+1-510-643-0930, Fax :642-4778 and E-mail iglesia@cchem.berkeley.edu

Abstract: Fischer-Tropsch synthesis (FTS) rates and selectivities were measured on iron-based catalysts promoted by Cu, K, or Ru at low H_2/CO ratios typical of coal- or biomass-derived synthesis gas. These catalysts were prepared via precipitation, drying in the presence of surface-active agent, and optimal promotion and activation protocols. C_{5+} selectivities were > 87 % (CO_2-free basis) and CO conversion rates were > 6.7 mol/h.g-at. Fe at 2.14 MPa and 508 K; these rates were larger than any reported previously for Fe-based FTS catalysts at these conditions.

Keywords: Fischer-Tropsch synthesis, Iron-based catalyst, hydrogen-poor synthesis gas

Introduction

The Fischer-Tropsch synthesis (FTS) converts synthesis gas mixtures derived from coal or natural gas into useful fuels and petrochemicals using Fe- and Co-based catalysts.[1, 2] Co-based catalysts are used for reactants derived from natural gas because of their low water-gas shift activity. Fe-based catalysts are able to reject O-atoms from CO as both H_2O and CO_2 and are thus better suited for synthesis gas streams with low H_2/CO ratios. Fe-based catalysts typically show much lower FT synthesis rates and C_{5+} selectivities than Co-based catalysts.

Fe-based catalysts with CO conversion, hydrocarbon formation rate, and selectivities similar to those on cobalt-based catalyst were recently reported.[3] These catalysts gave unprecedented activity and C_5^+ selectivity for stoichiometric synthesis gas (H_2/CO = 2) reactants. FTS catalysts with high catalytic activities with hydrogen-poor synthesis gas reactants (H_2/CO = 0.7-1) are needed to convert streams formed from coal or biomass. Here, we report FTS rates and selectivities on these materials with low hydrogen content reactants (H_2/CO = 1).

Experimental

Fe oxide precursors were prepared by co-precipitation from mixed solutions of Fe and Zn nitrates using $(NH_4)_2CO_3$.[3] Zinc (Zn/Fe=0.1) acts to prevent sintering without modifying chain growth selectivity. After coprecipitation, the powders were washed with surface-active agent (isopropyl alcohol). Isopropyl alcohol acts to prevent sintering of oxide precursors during drying and thermal treatments. K, Cu, and Ru promoters were added to precursors by incipient wetness impregnation (K/Fe=0.04-0.08, Cu(Ru)/Fe=0.00-0.06) and samples were treated in dry air at 543 K for 4 h. These catalysts were used as agglomerates with 100-180 μm diameters.

FTS reaction rates and selectivities were measured on catalysts (0.4 g) diluted with quartz in a fixed-bed single-pass flow reactor with plug-flow hydrodynamics after activation at 508-573 K and

0.1 MPa (H_2/CO= 1 or 2) for 0.1-6 h under synthesis gas stream before the FT reaction.[3] Reactant and product streams were analyzed by gas chromatography.

Results and discussion

FeZn oxides promoted with K and Cu (Cu/Fe=0.03 and K/Fe=0.06 atomic; Fe-Zn-Cu_3-K_6) showed the highest hydrocarbon productivity and C_5^+ selectivity at 508 K and 2.14 MPa among all catalysts prepared in this work. FTS performances on Fe-Zn-Cu_3-K_6 sample at several experimental conditions (temperature, pressure, H_2/CO ratio) are summarized in Table 1. Low H_2/CO reactants (H_2/CO = 1) led to low hydrocarbon productivities relative to those with stoichiometric reactants (H_2/CO = 2). Higher temperatures led to higher hydrocarbon productivities even at the lower reactant pressures used. Fe-Zn-Cu_3-K_6 samples are also compared with the most active reported Fe-based catalysts in Table 1 (at similar CO conversions, 50%).[4,5] Fe-Zn-Cu_3-K_6 showed the highest hydrocarbon productivity for FTS reaction among all reported catalysts, even though previously reported catalysts were tested with easier to convert stoichiometric streams.

Table 1 Steady State FTS performance of Various Fe-Based Catalysts under Synthesis Gas (H_2/CO = 1.0-2.0) Streams.

	Fe-Zn-Cu_3-K_6 (This work)			Fe-Zn-K_4-Cu_2 (3)	Fe-$Si_{4.6}$-K_4 (4)	Fe-SiO_2-$K_{5.9}$-$Cu_{4.4}$ (5)
Reactor Type	Fixed-bed			Fixed-bed	Slurry	Spinning Basket
Temperature (K)	508	543	508	508	543	523
Pressure (MPa)	2.14	1.31	2.14	2.14	1.31	2.4
H_2/CO ratio	1.0	1.0	2.0	2.0	1.7	2.0
CO space velocity	3.1	10.0	3.7	3.4	5.7	2.4 *
CO conversion (%)	52.2	51.4	47.8	50.8	50.0*	52.7
CO_2 selectivity (%)	36.6	41.1	28.1	31.7	40.0*	42.3*
CO rate (mol CO/h.g-cat)	0.07	0.23	0.08	0.08	0.12*	0.05*
Hydrocarbon productivity (g/h.kg-cat)	645	1911	789	765	1008	404

* Values calculated based on reported data or graphs.

Conclusion

The use of surface-active alcohol during the synthesis of oxide precursors, and optimal promotion and activation protocols led to high CO conversion rates and C_5^+ selectivities. The Fe-based catalysts promoted by Cu, K or Ru exhibit high catalytic activities with hydrogen-poor synthesis gas reactant (H_2/CO = 1). Fe-Zn-Cu_3-K_6 sample shows the highest hydrocarbon productivity and C_5^+ selectivity for FTS reaction among all reported catalysts.

References

[1] F. Fischer and H. Tropsch, Brennstoff-Chem. 7 (1926) 97.

[2] M. E. Dry, The Fischer-Tropsch Synthesis, Catal. Sci. Technol., Vol. 1, eds. J. R. Anderson and M. Boudart (Springer, New York, 1981) Chapter 4.

[3] S. Li, S. Krishnamoorthy, A. Li, G. D. Meitzner and E. Iglesia, J. Catal. 206 (2002) 202.

[4] A. P. Raje and B. H. Davis, Catal. Today 36 (1997) 335.

[5] G. P. Van der Laan and A. A. C. M. Beenackers, Ind. Eng. Chem. Res. 38 (1999) 1277.

Abstract submitted to "AIChE 2006 Annual Meeting San Francisco" November 12-17, 2006

Iron-Catalyzed Fischer-Tropsch Synthesis: Mechanism and Catalyst Optimization

Manuel Ojeda, Akio Ishikawa and Enrique Iglesia

Department of Chemical Engineering, University of California, Berkeley, CA 94720.

Abstract

The sequence in which promoters (K, Cu, Ru) are introduced into to Fe-Zn oxide precursors influences the uniformity of the promoter distribution and the reactivity of these materials in the Fischer-Tropsch synthesis (FTS). Impregnation with Cu^{2+} solutions and thermal treatment before K impregnation prevents recrystallization processes prevalent when this sequence is reversed. The resulting materials catalyze FTS with rates and selectivity similar to those on Co-based catalysts. A detailed kinetic study on the most active catalysts suggests that kinetically-relevant CO activation occurs via two parallel paths on CO-covered surfaces. On Fe catalysts, direct CO dissociation occurs on vicinal free sites and leads to the rejection of chemisorbed oxygen as CO_2 via subsequent reactions with chemisorbed CO. CO can also dissociate via reactions with chemisorbed hydrogen atoms in a step that rejects oxygen as H_2O; alkali promoters appear to favor direct CO dissociation, while Co surfaces dissociate CO predominantly via H-aided pathways with the exclusive formation of H_2O as the oxygen carrier. The effects of H_2 and CO and of using CO/D_2 reactants on FTS rates are consistent with this mechanistic proposal, which accounts also for the rate at which H_2O is converted to H_2 via secondary water-gas shift reactions.